A COMPARISON STUDY ON ACTUATOR TOPOLOGY OPTIMIZATION DESIGNS USING THE CONTROLLABILITY GRAMIAN

Juliano Fagundes Gonçalves

Daniel Milbrath De Leon

Jun Sérgio Ono Fonseca

juliano.fagundes@ufrgs.br

daniel.leon@ufrgs.br

jun@ufrgs.br

Department of Mechanical Engineering, Federal University of Rio Grande do Sul.

Rua Sarmento Leite 425, 90050-170, Porto Alegre, RS, Brazil.

Abstract. *This work compares methodologies for the optimal design of actuators for the vibration control of flexible structures. The goal is to find the location of actuators which maximizes the system controllability. A topology optimization was formulated to distribute two material phases in the domain: a passive linear elastic material and an active linear piezoelectric material. Different objective functions were implemented: smallest eigenvalue and trace of the controllability Gramian for an LQR control system. Analytical sensitivities for the finite element model are derived for the objective functions and constraints. Results are presented for vibration control of a two-dimensional short beam.*

Keywords: *Actuator placement, Topology optimization, Controllability Gramian.*

1 INTRODUCTION

The use of piezoelectric materials on vibration suppression of structures can be explained by their fast response and the possibility to be used as both sensor and actuator. Moreover, they are lightweight and can be bonded (or embedded) to many types of structures (Bruant et al., 2001). Sensors and actuators (S/A) placement is an important step in control design. For a simple structure, the S/A placement can be determined through engineer experience or trial and error analysis. However, several authors have been developing systematic methodologies to solve this problem. The controllability and observability tests cannot be directly applied in S/A placement problems due to their binary characteristics. Therefore, measures that quantify the degree of controllability and observability for a given system are required. Hamdan and Nayfeh (1989), introduced a geometrical interpretation for the Popov-Belevitch-Hautus (PBH) eigenvectors test. Junkins and Kim (1991), proposed a modal cost which represent the relevance of input and state vectors components. The relation between the controllability Gramian and the energy which is transmitted from the actuators to the structure was analyzed by Hac and Liu (1993). The Gramian approaches indicate that the maximization of some norm of this matrix could contribute for an improvement on the controllability.

Not only a controllability measure (CM) needs to be chosen, but also an optimal design methodology is required to solve the actuator placement problem. One can purely analyze a predefined set of actuators and compare their respective CM in order to define the best configuration. Several authors have used heuristic methods to find the optimum set of actuators from a set of candidates (Peng et al., 2005; Sohn et al., 2011). Silveira et al. (2015) proposed a methodology for topology optimization of actuators aiming to find the distribution of piezoelectric material which maximizes the system controllability.

In this work, a topology optimization for actuator placement is implemented based on the methodology proposed by Silveira et al. (2015), which considered the trace of controllability Gramian as objective function. Although the latter work has obtained successful designs, a large trace does not necessarily imply a non-singular Gramian which is required for a system to be completely state controllable. Hence, it is proposed a formulation where the smallest eigenvalue of controllability Gramian is maximized. This condition ensures that all states will be controllable.

2 COUPLED FINITE ELEMENT MODEL

In this work, the structure is composed by two different materials: a linear elastic and a linear piezoelectric. For the proposed problem, the coupled finite element model is given by:

$$\mathbf{M}_{uu}\ddot{\mathbf{u}} + \mathbf{K}_{uu}\mathbf{u} + \mathbf{K}_{u\phi}\boldsymbol{\phi} = \mathbf{f}, \tag{1}$$

$$\mathbf{K}_{u\phi}^{\mathrm{T}}\mathbf{u} + \mathbf{K}_{\phi\phi}\boldsymbol{\phi} = \mathbf{q}, \tag{2}$$

where $\mathbf{u}$ and $\boldsymbol{\phi}$ are, respectively, global vectors of mechanical and electrical degrees of freedom; $\mathbf{M}_{uu}$, $\mathbf{K}_{uu}$, $\mathbf{K}_{u\phi}$ and $\mathbf{K}_{\phi\phi}$ are mass, stiffness, piezoelectric coupling and dielectric capacitance global matrices, respectively; $\mathbf{f}$ is the global vector of external mechanical forces; and $\mathbf{q}$ is the global vector of electrical charges.

This model can be defined in modal coordinates. Therefore, the equation system is reduced, which is desirable when analyzing complex structures through the finite element method. Moreover, the truncation on mode m can be used in order to obtain a reduced modal model. A truncated modal matrix $\boldsymbol{\Psi}$ is used in the transformation from the generalized nodal coordinates $\mathbf{u}$ to the modal coordinates $\boldsymbol{\eta}$. If the full model is stable, this reduction always produces a stable reduced model. However, a feedback control system based on a truncated model is not necessarily stable for the residual modes, causing undesirable effects known as spillover (Gawronski, 2004). The electrical degrees of freedom $\boldsymbol{\phi}$ are used as active electrical known inputs to the actuator in the control system. Therefore, the term regarding the piezoelectric coupling term can be considered as an external force. Assuming a structural viscous damping model to the flexible structure, the truncated damped model of the structure with piezoelectric actuators can be written as:

$$\ddot{\boldsymbol{\eta}} + 2\mathbf{Z}\boldsymbol{\Omega}\dot{\boldsymbol{\eta}} + \boldsymbol{\Omega}^2\boldsymbol{\eta} = -\boldsymbol{\Psi}^{\mathrm{T}}\mathbf{K}_{u\phi}\boldsymbol{\phi} + \boldsymbol{\Psi}^{\mathrm{T}}\mathbf{f}, \tag{3}$$

where $\boldsymbol{\Omega}$ and $\mathbf{Z}$ are diagonal matrices of natural frequencies and modal damping, respectively, considering only the m first modes.

3 CONTROL METHODOLOGY

3.1 Modal model in state-space representation

The state-space representation carries information about the internal structure of the model. A state contains the minimal number of physical variables that allows calculating uniquely the output using the applied input. A linear time-invariant system is described by the following linear constant coefficient differential equations (Gawronski, 2004):

$$\dot{\mathbf{x}} = \mathbf{A}\mathbf{x} + \mathbf{B}_{\phi}\mathbf{u}^{\mathrm{c}}, \tag{4}$$

$$\mathbf{y} = \mathbf{C}\mathbf{x}, \tag{5}$$

where $\mathbf{x}$ is the state vector, $\mathbf{u}^{\mathrm{c}}$ is the system input vector, and $\mathbf{y}$ is the system output vector; $\mathbf{A}$, $\mathbf{B}_{\phi}$, and $\mathbf{C}$ are the system, input and output matrices, respectively.

In this work, the truncated modal displacements and velocities are used as state variables, thus a vector of state variables $\mathbf{x}$ can be written as:

$$\mathbf{x} = \left\{ \begin{array}{c} \eta \\ \dot{\eta} \end{array} \right\}. \tag{6}$$

Therefore, the open-loop system represented in Eq. (4) can be fully determined, disregarding the external mechanical forces, through the electrical input vectors $\mathbf{u}^{\mathrm{c}} = [\mathbf{0} \quad \boldsymbol{\phi}]^{\mathrm{T}}$, and the system and electrical input matrices, given by:

$$\mathbf{A} = \begin{bmatrix} \mathbf{0} & \mathbf{I} \\ -\mathbf{\Omega}^2 & -2\mathbf{Z}\mathbf{\Omega} \end{bmatrix}, \quad \mathbf{B}_\phi = \begin{bmatrix} \mathbf{0} \\ -\mathbf{\Psi}^{\mathrm{T}}\mathbf{K}_{u\phi} \end{bmatrix}. \tag{7}$$

3.2 Controllability Gramian

In control theory, controllability measures the ability of a particular set of actuators to control all the states of a system. For an asymptotically stable system, i.e., if all poles (eigenvalues) of $\mathbf{A}$ have negative real part, the system response is limited and the covariance matrix for steady state is bounded (Preumont, 2002). Thus, considering a general set of parameters in state-space $(\mathbf{A}, \mathbf{B})$, the system response to a group of independent white noise of unit intensity is given by:

$$\mathbf{W}_c = \int_0^\infty e^{\mathbf{A}\tau}\, \mathbf{B}\mathbf{B}^{\mathrm{T}}\, e^{\mathbf{A}^{\mathrm{T}}\tau}\, d\tau, \tag{8}$$

which is called Controllability Gramian. For a general time-invariant system, as Eq. (4), one can also obtain the Controllability Gramian from the Lyapunov equation (Gawronski, 2004):

$$\mathbf{A}\mathbf{W}_c + \mathbf{W}_c\mathbf{A}^{\mathrm{T}} + \mathbf{B}\mathbf{B}^{\mathrm{T}} = \mathbf{0}. \tag{9}$$

The system is completely controllable if all states can be excited by the control input. This condition is fully satisfied if and only if $\mathbf{W}_c$ is positive definite (Preumont, 2002).

4 TOPOLOGY OPTIMIZATION FOR ACTUATOR DESIGN

4.1 Proposed formulation

The material model used in this work includes two solid phases: isotropic elastic and piezoelectric materials. The model that defines the effective properties of the interpolated material is given by:

$$[\mathbf{c}^E] = \boldsymbol{\rho}^{p1}[\mathbf{c}^E_{pzt}] + (1 - \boldsymbol{\rho}^{p1})[\mathbf{c}^E_{elas}], \tag{10}$$

$$[\mathbf{e}] = \boldsymbol{\rho}^{p2}[\mathbf{e}_{pzt}], \tag{11}$$

$$[\boldsymbol{\epsilon}^S] = \boldsymbol{\rho}^{p2}[\boldsymbol{\epsilon}^S_{pzt}], \tag{12}$$

$$\gamma = \boldsymbol{\rho}\gamma_{pzt} + (1 - \boldsymbol{\rho})\gamma_{elas}, \tag{13}$$

where $[\mathbf{c}^E_{elas}]$, and $[\mathbf{c}^E_{pzt}]$ are the elastic properties of base (purely elastic isotropic) and piezoelectric material, respectively; $[\mathbf{e}_{pzt}]$ and $[\boldsymbol{\epsilon}^S_{pzt}]$ define the electromechanical coupling and dielectric properties of the piezoelectric material. γ_{elas} and γ_{pzt} are the specific weight for each material.

Through this interpolation, it is defined that elastic isotropic material is obtained when $\rho = 0$ and piezoelectric material is obtained when $\rho = 1$.

In order to enable the interpretation of the optimal actuator placement, it is desirable the structure presents either the fully properties of a piezoelectric or base (elastic isotropic) material. To that matter, the intermediate values of the design variable ρ_i are penalized by the exponents $p1$ and $p2$, so that can be forced toward either 0 or 1.

The controllability Gramian must be maximized in order to have the optimal location of active piezoelectric material (actuators). Moreover, the resulting system must be completely controllable, i.e., all states should be excited and controlled by the actuators. Taking into consideration these preliminary requirements, it is proposed the following optimization formulation:

$$\min_{\boldsymbol{\rho}} \quad (-\lambda_1)\,, \tag{14}$$

$$\text{subject to} \begin{cases} V = \dfrac{\int_\Omega \boldsymbol{\rho}\, d\Omega}{\int_\Omega d\Omega} \leq V^{\max}, \\ \qquad\quad 0 \leq \boldsymbol{\rho} \leq 1, \end{cases} \tag{15}$$

where λ_1 is the smallest eigenvalue of $\mathbf{W}_c$, $\boldsymbol{\rho}$ is a vector of design variables, V is the normalized piezoelectric material volume, Ω is the three-dimensional domain, and V^{max} is the volume constraint.

In order to solve the optimization problem, sequential linear programming (SLP) was used. For the optimization process, it was considered 8% for the volume constraint and cubic penalization. Following the convergence criteria, the iterative process stops when the maximum change of design variables between two successive iterations is less than 2%. As any nonconvex optimization problem, one can guarantee only local minima. However, the initial cases converged to the same results under different initial conditions.

4.2 Sensitivity analysis

In order to find the optimal set of design variables, an SLP algorithm is used.. As a first order method, it requires the sensitivities of the objective function and constraints with respect to design variables. For this choice of objective functions and constraints, the sensitivities were analytically derived.

The controllability Gramian sensitivity can be obtained differentiating the Lyapunov equation presented in Eq. (9) with respect to design variables $\boldsymbol{\rho}$:

$$\frac{\partial \mathbf{A}}{\partial \boldsymbol{\rho}}\mathbf{W}_c + \mathbf{A}\frac{\partial \mathbf{W}_c}{\partial \boldsymbol{\rho}} + \frac{\partial \mathbf{W}_c}{\partial \boldsymbol{\rho}}\mathbf{A}^{\mathrm{T}} + \mathbf{W}_c\frac{\partial \mathbf{A}^{\mathrm{T}}}{\partial \boldsymbol{\rho}} + \frac{\partial \mathbf{B}}{\partial \boldsymbol{\rho}}\mathbf{B}^{\mathrm{T}} + \mathbf{B}\frac{\partial \mathbf{B}^{\mathrm{T}}}{\partial \boldsymbol{\rho}} = \mathbf{0}. \tag{16}$$

An effective way to design a feedback control system is to use the optimal linear quadratic regulator (LQR). This is the simplest and the most frequently used formulation. A linear state feedback is evaluated with constant gain $\mathbf{u}^{\mathrm{c}} = -\mathbf{G}\mathbf{x}$ in a way that a quadratic cost functional J is minimized (Preumont, 2002):

$$J = \frac{1}{2}\int_0^{t_f} \left(\mathbf{x}^{\mathrm{T}}\mathbf{Q}\mathbf{x} + \mathbf{u}^{\mathrm{c}\mathrm{T}}\mathbf{R}\mathbf{u}^{\mathrm{c}}\right) dt, \tag{17}$$

where $\mathbf{Q}$ is a positive semi-definite weighting matrix for the state variables and $\mathbf{R}$ is a positive definite weighting matrix for the control inputs.

The LQR control theory is considered in steady state, then the feedback gain matrix is given by $\mathbf{G} = \mathbf{R}^{-1}\mathbf{B}_{\phi}{}^{\mathrm{T}}\mathbf{P}$, where the matrix $\mathbf{P}$ is the solution of the algebraic Riccati equation:

$$\mathbf{A}^{\mathrm{T}}\mathbf{P} + \mathbf{P}\mathbf{A} - \mathbf{P}\mathbf{B}_{\phi}\mathbf{R}^{-1}\mathbf{B}_{\phi}{}^{\mathrm{T}}\mathbf{P} + \mathbf{Q} = \mathbf{0}. \tag{18}$$

Considering the previous assumptions, the input control matrix $\mathbf{B}$ used in Eq. (16) is defined by $\mathbf{B} = -\mathbf{B}_{\phi}\mathbf{G}$. Since all terms of Eq. (16) excepting the $\partial\mathbf{W}_c/\partial\boldsymbol{\rho}$ are known, this sensitivity of controllability Gramian can be find by solving a new Lyapunov equation. For this, the sensitivities of the state-space parameters $\mathbf{A}$ and $\mathbf{B}$ with respect to design variables are required. These derivatives are given by:

$$\frac{\partial\mathbf{A}}{\partial\boldsymbol{\rho}} = \begin{bmatrix} \mathbf{0} & \mathbf{0} \\ -\frac{\partial\boldsymbol{\Omega}^2}{\partial\boldsymbol{\rho}} & -2\mathbf{Z}\frac{\partial\boldsymbol{\Omega}}{\partial\boldsymbol{\rho}} \end{bmatrix}, \tag{19}$$

and,

$$\frac{\partial\mathbf{B}}{\partial\boldsymbol{\rho}} = -\frac{\partial\mathbf{B}_{\phi}}{\partial\boldsymbol{\rho}}\mathbf{G} - \mathbf{B}_{\phi}\frac{\partial\mathbf{G}}{\partial\boldsymbol{\rho}}. \tag{20}$$

The derivatives of $\mathbf{B}_{\phi}$ and $\mathbf{G}$ are obtained by:

$$\frac{\partial\mathbf{B}_{\phi}}{\partial\boldsymbol{\rho}} = \begin{bmatrix} \mathbf{0} \\ -\frac{\partial\boldsymbol{\Psi}^{\mathrm{T}}}{\partial\boldsymbol{\rho}}\mathbf{K}_{u\phi} - \boldsymbol{\Psi}^{\mathrm{T}}\frac{\partial\mathbf{K}_{u\phi}}{\partial\boldsymbol{\rho}} \end{bmatrix}, \tag{21}$$

and,

$$\frac{\partial\mathbf{G}}{\partial\boldsymbol{\rho}} = \frac{\partial\mathbf{R}^{-1}}{\partial\boldsymbol{\rho}}\mathbf{B}_{\phi}^{\mathrm{T}}\mathbf{P} + \mathbf{R}^{-1}\frac{\partial\mathbf{B}_{\phi}^{\mathrm{T}}}{\partial\boldsymbol{\rho}}\mathbf{P} + \mathbf{R}^{-1}\mathbf{B}_{\phi}^{\mathrm{T}}\frac{\partial\mathbf{P}}{\partial\boldsymbol{\rho}}. \tag{22}$$

From the Riccati equation for steady state, the partial derivative $\partial\mathbf{P}/\partial\boldsymbol{\rho}$ is obtained by solving the following Lyapunov equation (Silveira et al., 2015):

$$\mathbf{A}_{\mathrm{c}}^{\mathrm{T}}\frac{\partial \mathbf{P}}{\partial \boldsymbol{\rho}} + \frac{\partial \mathbf{P}}{\partial \boldsymbol{\rho}}\mathbf{A}_{\mathrm{c}} + \mathbf{P}\left(\frac{\partial \mathbf{A}}{\partial \boldsymbol{\rho}} + \frac{\partial \mathbf{B}_{\phi}}{\partial \boldsymbol{\rho}}\mathbf{G}\right) + \left(\frac{\partial \mathbf{A}^{\mathrm{T}}}{\partial \boldsymbol{\rho}} + \mathbf{G}^{\mathrm{T}}\frac{\partial \mathbf{B}_{\phi}^{\mathrm{T}}}{\partial \boldsymbol{\rho}}\right)\mathbf{P} = \mathbf{0}, \tag{23}$$

where $\mathbf{A}_{\mathrm{c}} = \mathbf{A} - \mathbf{B}_{\phi}\mathbf{G}$ is the closed loop system matrix.

Finally, in order to calculate the controllability Gramian sensitivity through Eq. (16), $\partial \mathbf{K}_{u\phi}/\partial \boldsymbol{\rho}$ is required. This sensitivity is obtained from the piezoelectric coupling elemental matrix:

$$\frac{\partial \mathbf{K}_{u\phi}^{e}}{\partial \boldsymbol{\rho}} = \int_{\Omega^{e}} \mathcal{B}_{u}^{\mathrm{T}}\frac{\partial [\mathbf{e}]^{\mathrm{T}}}{\partial \boldsymbol{\rho}}\mathcal{B}_{\phi} d\Omega, . \tag{24}$$

where $\mathcal{B}_u$ and $\mathcal{B}_\phi$ are respectively the matrices that relate mechanical strain with displacement, and electric field with electric potential. The sensitivities of the material model, presented in Eqs. (10) to (13), with respect to design variable $\boldsymbol{\rho}$, can be easily obtained. Likewise, other derivatives such as mechanical stiffness and mass matrices can be derived.

It is also required the sensitivity of both modal and Gramian eigenvalues. Considering a real and symmetric eigenvalues problem:

$$\left(\mathbf{K}_{uu} - \omega_j^2\mathbf{M}_{uu}\right)\boldsymbol{\psi}_j = \mathbf{0}, \tag{25}$$

$$\boldsymbol{\psi}_j^{\mathrm{T}}\mathbf{M}_{uu}\boldsymbol{\psi}_j = 1, \qquad j = 1, 2, ..., n, \tag{26}$$

where ω_j^2 is the j-th eigenvalue; $\boldsymbol{\psi}_j$ is its respective eigenvector; n is the number of degrees of freedom. The eigenvalue sensitivity can be obtained solving a new problem for $\partial \omega_j^2/\partial \boldsymbol{\rho}$:

$$\left[\boldsymbol{\Psi}^{\mathrm{T}}\left(\frac{\partial \mathbf{K}_{uu}}{\partial \boldsymbol{\rho}} - \omega_j^2\frac{\partial \mathbf{M}_{uu}}{\partial \boldsymbol{\rho}}\right)\boldsymbol{\Psi} - \frac{\partial \omega_j^2}{\partial \boldsymbol{\rho}}\mathbf{I}\right]\gamma_j = \mathbf{0}, \tag{27}$$

considering m repeated eigenvalues ω_j^2 , $j = 1, 2, ..., m$, where $m \leq n$; and the matrix composed by the eigenvectors $\boldsymbol{\Psi} = [\boldsymbol{\psi}_1, \boldsymbol{\psi}_2, ..., \boldsymbol{\psi}_m]$. If there are only distinct eigenvalues, this equation can be simplified. For the Gramian, the same procedure can be employed, considering the problem written as:

$$\left(\mathbf{W}_c - \lambda_j\mathbf{I}\right)\boldsymbol{\chi}_i = \mathbf{0} \tag{28}$$

where $\mathbf{I}$ is the identity matrix, λ_j is the j-th eigenvalue of $\mathbf{W}_c$, and $\boldsymbol{\chi}_i$ is its respective eigenvector. For the eigenvector derivatives, it was used the methodology proposed by Wu (2007) taking into consideration the possibility of both distinct and repeated eigenvalues.

5 RESULTS AND DISCUSSIONS

5.1 Numerical example

The tests were performed for a cantilever beam with rectangular cross section, Fig. 1, measuring $600\text{mm} \times 150\text{mm} \times 20\text{mm}$. It was discretized using 600 $(50 \times 12 \times 1)$ 8-node brick nonconforming finite elements (Taylor et al., 1976) presenting three mechanical and one electrical degrees of freedom per node. In this particular study, only in-plane vibration modes are considered and controlled. In this work, control systems considering one independent electrode are considered.

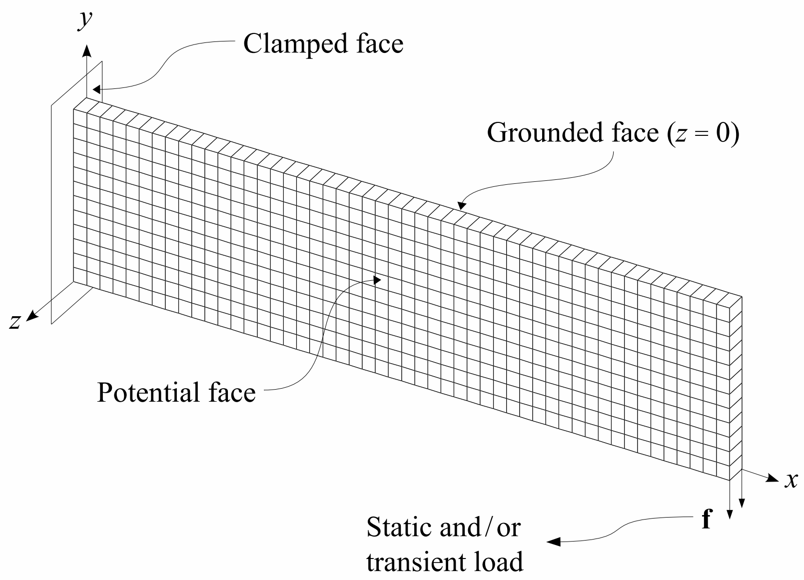

Figure 1: Finite element mesh and boundary conditions.

The constitutive properties of the isotropic elastic material (aluminum) and the piezoelectric material (PZT5A), polarized in z-direction, are shown in Tables 1 and 2. For this particular case, the piezoelectric effect responsible for the vibration control is provided from the d31-mode.

Table 1: Elastic material properties.

ALUMINUM	
Young's modulus	$71 \cdot 10^9\ \text{N/m}^2$
density	$2700\ \text{kg/m}^3$
Poisson's ratio	0.33

For the dynamic analysis, modal damping ratios of 1.71%, 0.72%, 0.42% and 0.41% were assumed for the first modes (Vasques and Rodrigues, 2006).

Table 2: Piezoelectric material properties.

PZT5A	
elastic constants	$(10^{10}\ \mathrm{N/m^2})$
c_{11}^E	12.1
c_{12}^E	7.54
c_{13}^E	7.52
c_{33}^E	11.1
c_{44}^E	2.11
c_{66}^E	2.26
piezoelectric constants	$(\mathrm{C/m^2})$
e_{31}	-5.4
e_{33}	15.8
e_{51}	12.3
dielectric constants	$(\mathrm{F/m})$
ϵ_0	$8.85 \cdot 10^{-12}$
ϵ_{11}/ϵ_0	916
ϵ_{33}/ϵ_0	830
density	$7750\ \mathrm{kg/m^3}$

5.2 Optimal distribution of piezoelectric material

The actuator placement can be defined by interpreting the piezoelectric material distribution. This distribution is presented in Fig. 2 for cases where the first vibration mode is considered in the control system. The solutions obtained maximizing smallest eigenvalue and trace of controllability Gramian are very similar when only the first mode is considered.

Case 1:

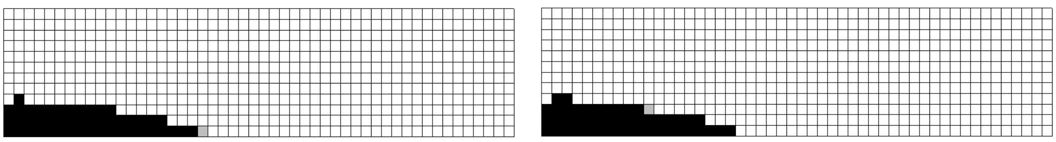

(a) (b)

Figure 2: Optimal topology for 1 mode: maximizing (a) smallest eigenvalue and (b) trace of $\mathbf{W}_c$.

Figure 3 presents optimal solutions for cases considering both first and second vibration modes in the control system. Naturally, this is the most complex case for vibration control since there is only one input and two states to be controlled. For this case, when maximizing λ_1, there is a small distribution of piezoelectric material on the free-tip of the beam, although it seems to be a not effective region regarding the vibration control.

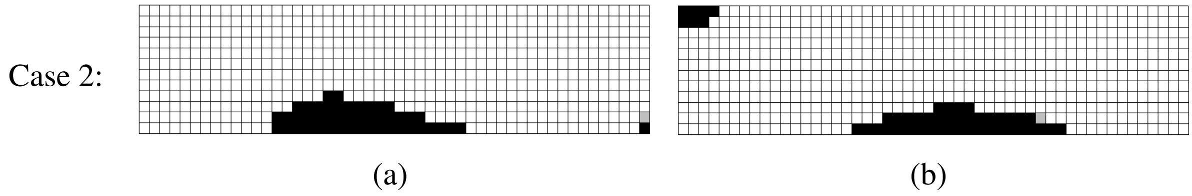

Figure 3: Optimal topology for 2 modes: maximizing (a) smallest eigenvalue and (b) trace of $\mathbf{W}_c$.

5.3 Objective functions convergence

The convergences of the objective functions for the case considering two modes in the control system are presented in Fig. 4. For this case, the use of the smallest eigenvalue of $\mathbf{W}_c$ as objective function results in a slightly slower convergence.

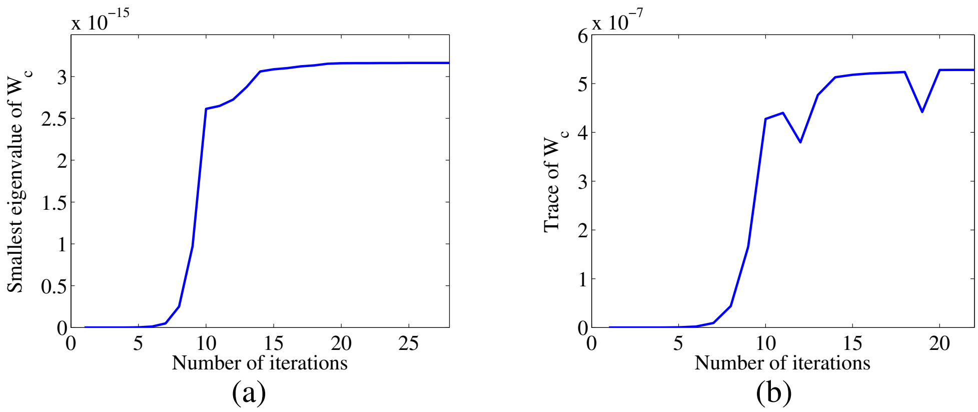

Figure 4: Convergence of objective functions for case 2.

5.4 Unit step response

In order to compare the dynamic response of the structure, an external unit force applied on the free-tip of the beam was considered. Three dynamic responses are shown: with no control (Open-loop), with LQR control based on the optimal topology obtained through the maximization of the smallest eigenvalue of $\mathbf{W}_c$, and with LQR control based on the optimal topology obtained through the maximization of the trace of $\mathbf{W}_c$.

This work omits responses for case 1, where only the first mode is controlled, since there is no significantly difference when maximizing the smallest eigenvalue or the trace of $\mathbf{W}_c$.

Figure 5 presents the displacement on the free-tip of the beam for case 2, which intend to control the first and the second vibration modes. The open-loop response in this figure was obtained for the structure which the Gramian trace was maximized. Although there is a slight difference of structural dynamics for the two structures, it can be noticed that both settling time and amplitude are reduced when the smallest eigenvalue of $\mathbf{W}_c$ is used as objective function.

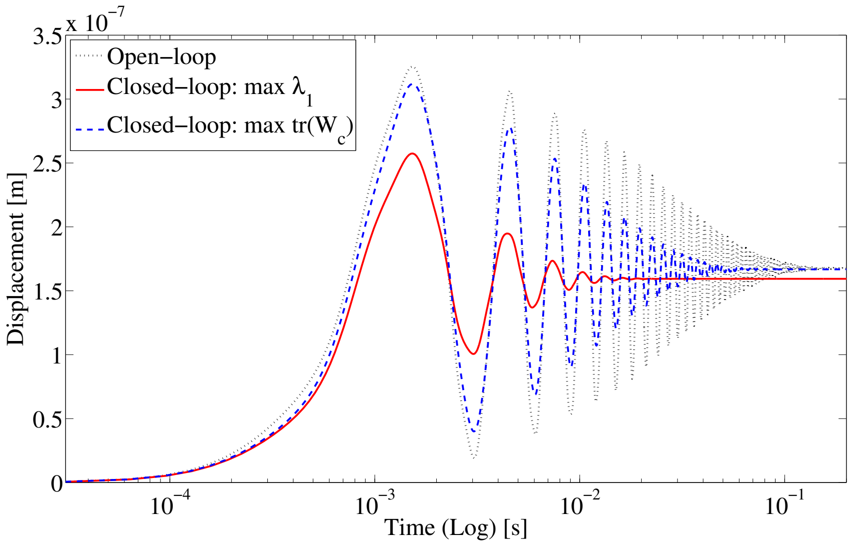

Figure 5: Unit step response for case 2.

6 FINAL REMARKS

The actuator placement problem was solved by the maximization of the controllability Gramian. Two different formulations for the topology optimization were implemented: maximization of smallest eigenvalue and trace of the controllability Gramian. In order to compare these formulations, a unit step response was evaluated for both closed-loop cases and for an open-loop case. When only the first mode is considered in the control system, both formulations are the same due to the state vector chosen which has dependent terms. For the case where the first and the second modes are considered, the results present an important difference regarding the controllability measure used as objective function. The optimization using the smallest eigenvalue of $\mathbf{W}_c$ focuses on the control of the less controllable state. However, for this example structure and for the analyzed cases, the maximization of one controllability measure contributes to an improvement in the other. Consequently, all solutions, regardless the measure used, result in completely controllable systems.

ACKNOWLEDGEMENTS

The authors would like to acknowledge the financial support by CNPq and CAPES.

REFERENCES

Bruant, I., Coffignal, G., Lene, F. & Verge, M., 2001. A methodology for determination of piezoelectric actuator and sensor location on beam structures. *Journal of sound and vibration*, vol. 243, n. 5, pp. 861-882.

Gawronski, W. K., 2004. *Advanced structural dynamics and active control of structures*, Springer, New York.

Hac, A. & Liu, L., 1993. Sensor and actuator location in motion control of flexible structures. *Journal of Sound and Vibration*, vol. 167, n. 2, pp. 239-261.

Hamdan, A. & Nayfeh, A., 1989. Measures of modal controllability and observability for first- and second-order linear systems. *Journal of guidance, control, and dynamics*, vol. 12, n. 3, pp. 421-428.

Junkins, J. L. & Kim, Y., 1991. Measure of controllability for actuator placement. *Journal of Guidance, Control, and Dynamics*, vol. 14, n. 5, pp. 895-902.

Peng, F., Ng, A. & Hu, Y., 2005. Actuator placement optimization and adaptive vibration control of plate smart structures. *Journal of Intelligent Material Systems and Structures*, vol. 16, n. 3, pp. 263-271.

Preumont, A., 2002. *Vibration control of active structures, An introduction*, Kluwer, Amsterdam.

Silveira, O. A. A., Fonseca, J. S. O. & Santos, I. F., 2015. Actuator topology design using the controllability Gramian. *Structural and Multidisciplinary Optimization*, vol. 51, n. 1, pp. 145-157.

Sohn, J. W., Choi, S. & Kim, H. S., 2011. Vibration control of smart hull structure with optimally placed piezoelectric composite actuators. *International Journal of Mechanical Sciences*, vol. 53, n. 8, pp. 647-659.

Taylor, R. L., Beresford, P. J. & Wilson, E. L., 1976. A non-conforming element for stress analysis. *International Journal for Numerical Methods in Engineering*, vol. 10, n. 6, pp. 1211-1219.

Vasques, C. M. A. & Rodrigues, J. D., 2006. Active vibration control of smart piezoelectric beams: Comparison of classical and optimal feedback control strategies. *Computers & structures*, vol. 84, n. 22, pp. 1402-1414.

Wu, B., Xu, Z. & Li, Z., 2007. A note on computing eigenvector derivatives with distinct and repeated eigenvalues. *Communications in numerical methods in engineering*, vol. 23, n. 3, pp. 241-251.